

## Transient behaviour of perovskite-based monolithic reactors in the catalytic combustion of methane

Stefano Cimino<sup>a</sup>, Almerinda Di Benedetto<sup>b</sup>, Raffaele Pirone<sup>b,\*</sup>, Gennaro Russo<sup>b</sup>

<sup>a</sup> *Dipartimento di Ingegneria Chimica, Università degli Studi di Napoli "Federico II" Napoli, Italy*

<sup>b</sup> *Istituto Ricerche sulla Combustione — CNR, P.le Tecchio 80, 80125 Napoli, Italy*

### Abstract

The transient behaviour of perovskite-based catalysts prepared via active phase dispersion on La/ $\gamma$ -Al<sub>2</sub>O<sub>3</sub> washcoated cordierite monoliths has been investigated in the autothermal combustion of lean methane mixtures. During start-up and shut-down operations, the reaction front moves from the outlet towards the inlet (ignition) or vice versa (extinction), with a time scale significantly higher than space time. The CH<sub>4</sub>/O<sub>2</sub>/N<sub>2</sub> feed mixture is completely converted to CO<sub>2</sub> and H<sub>2</sub>O provided its inlet temperature is about 500°C, a value not affected by catalyst length and gas flow rate, the phenomenon being kinetically controlled. Gas flow rate significantly affects solid steady-state temperature, as at higher flow rates the thermal power produced by combustion is higher in comparison with heat losses by radiation and conduction and temperature rise is closer to the adiabatic value. The fresh catalysts weakly deactivate during the first 60 h of operation under reaction conditions, but after 120 h the activity is still very high and not significantly affected by further ageing. The transient behaviour of the system has been simulated by a mathematical model, characterised by an increased solid thermal conductivity to take into account the relevant contribution of internal radiation between channel surfaces. © 2001 Elsevier Science B.V. All rights reserved.

**Keywords:** Methane; Catalytic combustion; Perovskite; Monolith; Modelling

### 1. Introduction

Catalytic combustion of methane in structured reactors is an effective and clean technology for both adiabatic and radiant burners for industrial and domestic applications [1–6]. A considerable amount of research has been devoted in recent years to the study of materials, reactor configurations and operating conditions of interest for such processes [7]. The most investigated systems are constituted by PdO-based monoliths, generally obtained via noble metal deposition on a high surface area  $\gamma$ -Al<sub>2</sub>O<sub>3</sub> washcoat. Unfortunately,

this system is very expensive and not applicable to processes where temperature can rise well above 800°C. Relevant examples are fully catalytic combustors for gas turbine application under lean adiabatic conditions [2,3] and premixed non-adiabatic radiant burners [4–6]. Therefore, the development of catalytic materials other than noble metals with good activity in combustion reactions, but more heat resistant, is presently a growing challenge catalysis research.

We have recently investigated the catalytic properties in methane combustion of perovskite-based honeycomb monoliths. Perovskite-type mixed oxides with general formula ABO<sub>3</sub> have attracted great attention for combustion applications as an alternative to the very active noble metal-based catalysts, as they offer potential better features in terms of elevated

\* Corresponding author. Tel.: +39-081-768-2220;  
fax: +39-081-593-6936.  
E-mail address: pirone@irc.na.cnr.it (R. Pirone).

**Nomenclature**

$a_{\text{rad}}$	specific radiant external surface area ( $\text{m}^2/\text{m}^3$ )
$a_v$	gas solid surface per unit gas volume ( $\text{m}^2/\text{m}^3$ )
$a_{v,s}$	gas solid surface per unit solid volume ( $\text{m}^2/\text{m}^3$ )
$a_w$	specific surface area of wall ( $\text{m}^2/\text{m}^3$ )
$a_{wF}$	specific surface area of wall–oven ( $\text{m}^2/\text{m}^3$ )
$C_g$	total gas concentration ( $\text{mol}/\text{m}^3$ )
$C_{pg}, C_{ps}$	gas and solid heat capacity ( $\text{J}/(\text{kg K})$ )
$d$	diameter of monolith channel (m)
$D$	molecular diffusion ( $\text{m}^2/\text{s}$ )
$D_{\text{eff}}$	effective diffusion in the catalyst ( $\text{m}^2/\text{s}$ )
$E_{\text{act}}$	activation energy ( $\text{cal}/\text{mol}$ )
$h_g$	gas–solid heat transfer coefficient ( $\text{J}/\text{m}^2 \text{ s K}$ )
$\Delta H$	heat of reaction ( $\text{J}/\text{mol}$ )
$k_g$	gas–solid mass transfer coefficient ( $\text{m}/\text{s}$ )
$k_s$	kinetic constant ( $\text{m}^3/\text{kg}_{\text{cat}} \text{ s}$ )
$L$	reactor length (m)
$Nu$	Nusselt number
$P$	pressure (Pa)
$Pe$	Peclet number
$Pr$	Prandtl number
$R$	gas constant ( $\text{cal}/\text{mol K}$ )
$R_{\text{CH}_4}$	catalytic reaction rate ( $\text{s}^{-1}$ )
$Sc$	Schmidt number
$Sh$	Sherwood number
$t$	time (s)
$T_F$	oven temperature (K)
$T_g$	mean gas temperature (K)
$T_g^{\text{in}}$	inlet gas temperature (K)
$T_s^0$	initial catalyst temperature (K)
$T_s$	mean solid temperature (K)
$T_w$	mean temperature of surroundings (K)
$U_s$	global radial exchange coefficient per solid volume ( $\text{W}/\text{m}^3 \text{ K}$ )
$U_w$	global radial exchange coefficient per wall volume ( $\text{W}/\text{m}^3 \text{ K}$ )

$U_{wF}$	global radial exchange coefficient (wall–furnace) per wall volume ( $\text{W}/\text{m}^3 \text{ K}$ )
$v_g$	mean gas velocity (m/s)
$x_{\text{CH}_4}$	methane molar fraction in the gas phase
$x_{\text{CH}_4}^{\text{in}}$	methane inlet molar fraction in gas
$x_{\text{CH}_4}^s$	methane molar fraction on catalyst
$z$	axial position (m)

*Greek letters*

$\alpha$	solid thermal diffusivity
$\delta$	thermocouple lag
$\varepsilon$	catalyst emissivity
$\lambda_g$	gas thermal conductivity ( $\text{W}/\text{m K}$ )
$\lambda_s$	effective solid thermal conductivity ( $\text{W}/\text{m K}$ )
$\mu_g$	gas viscosity (Pa s)
$\rho_g$	gas density ( $\text{kg}/\text{m}^3$ )
$\rho_s$	apparent catalyst density ( $\text{kg}/\text{m}^3$ )
$\rho_w$	apparent catalyst density ( $\text{kg}/\text{m}^3$ )
$\sigma$	Stephan–Boltzmann constant ( $\text{W}/\text{m}^2 \text{ K}^4$ )
$\Phi$	Thiele modulus

chemical and thermal stability (up to  $1100^\circ\text{C}$ ) and mainly, lower cost accompanied by a good specific activity at moderate temperature [8,9]. The main limit to the application of perovskites is represented by their lower activity at low temperatures and strong tendency to sinter at temperatures higher than  $800^\circ\text{C}$  [10]. However, deposition of a  $\gamma\text{-Al}_2\text{O}_3$  washcoat (stabilised by the addition of  $\text{La}_2\text{O}_3$ ) on commercial cordierite monoliths and subsequent dispersion of  $\text{LaMnO}_3$  perovskitic active phase onto washcoat pores produces very active and stable catalysts [11], able to ignite a 3 vol.%  $\text{CH}_4/\text{air}$  mixture with a preheat temperature of about  $500^\circ\text{C}$ , working in a stable way for at least 50 h under combustion conditions at about  $1000^\circ\text{C}$  [12]. This system appears very promising for such kind of applications which take advantage from reaching temperature as high as  $1100^\circ\text{C}$ .

In this work, we have extended the study on these structured catalysts to their transient behaviour in lean premixed methane combustion with particular care to the effect of monolith length, reactants flow rate, long-term operation and preheating temperature

(ignition–extinction cycles). A 1D heterogeneous mathematical model has been developed in order to simulate the behaviour of the monolithic combustor, and assess the most relevant chemico-physical phenomena that determine catalyst temperature profile evolution during start-up operation.

## 2. Experimental

### 2.1. Catalyst preparation

Commercial cordierite monoliths (Corning) with a cell density of 400 cpsi were cut to obtain samples of two lengths (2.3 and 4.6 cm) with 25 channels on the cross-section. Monoliths were washcoated with alumina by repeated dipping in a slurry of finely grounded  $\gamma$ - $\text{Al}_2\text{O}_3$  powder and pseudoboehmite [11].  $\text{La}_2\text{O}_3$  (7 wt.%) was added to the washcoat by impregnation, while  $\text{LaMnO}_3$  active phase was dispersed on the monoliths using deposition–precipitation (DP) method with urea, as already reported in [11]. Several cycles were needed to reach target perovskite loading (30 wt.% with respect to the washcoat). After each cycle, the monoliths were calcined at 800°C in air for 3 h.

### 2.2. Catalytic activity measurements

Combustion experiments were carried out in a lab scale quartz reactor already described in [12], positioned inside a three zone electrical tubular furnace. The central channel was blocked for catalyst wall temperature measurement with K-type thermocouples ( $d = 0.5$  mm), two of which entering from the top and one from the bottom of the reactor. The number and position of thermocouples in the central monolith channel for the two different catalyst lengths investigated is as follows: three measurements for longer sample ( $T_1$ : 0.5 cm;  $T_2$ : 2.5 cm;  $T_3$ : 3.4 cm from the inlet section), two measurements for the 2.3 cm long catalyst ( $T_{\text{in}}$ : 0.5 cm;  $T_{\text{out}}$ : 1.5 cm). The axial position was determined by comparing gradations on the thermocouples against a length scale, with an accuracy estimated within  $\pm 1$  mm. Additional thermocouples were located both upstream of the catalyst and on its external side in order to evaluate inlet gas temperature and radial heat transfer effects, respectively. The gaseous flow rates were regulated by Brooks

5850 mass flow controllers and premixed at atmospheric pressure to obtain a feed containing 3 vol.%  $\text{CH}_4$ , 10 vol.%  $\text{O}_2$  (beyond minimum oxygen content (MOC) for safety reasons), balance  $\text{N}_2$ . Total flow rate was varied in the range 24–72  $\text{NL/h}$  corresponding to a GHSV 22 000–132 000  $\text{h}^{-1}$ , based on monolith volume. The feed and product streams were continuously analysed (after passing through  $\text{CaCl}_2$  trap) using an Hartmann&Braun advance optima apparatus equipped with five independent, non-dispersive infrared detectors for  $\text{CH}_4$  (high and low concentrations),  $\text{CO}_2$ ,  $\text{CO}$  and  $\text{NO}$ .

Transient experiments were conducted by first allowing a steady-state to be achieved without methane in the feed; then methane was added stepwise, while gas preheating temperature was either kept constant or varied at fixed rate ( $\leq 5^\circ\text{C/min}$ , heating or cooling). Transient temperature profiles at various positions in the monolith and product concentrations were contemporarily acquired and recorded on a PC as functions of time.

## 3. Results

The typical behaviour of the perovskite-based monolith during the ignition of combustion process is shown in Fig. 1, where the transient evolution of solid temperature profile, as measured in three different axial positions, together with that of methane conversion and  $\text{CO}$  selectivity are reported. The reactor works with a relatively cold  $\text{CH}_4/\text{O}_2/\text{N}_2$  feed mixture (about 500°C), which is able to autothermally sustain the higher temperature level reached by the monolithic catalyst (about 900°C in the axial position at 0.5 cm from the inlet section) by completely converting methane with negligible by-production of  $\text{CO}$ . However, the temperature rise of the system is lower than the adiabatic one (about 1250°C), due to significant heat dispersion by radiation, particularly relevant for the high value of surface to volume ratio characteristic of the small scale monolithic reactor.

Fig. 1 clearly shows that ignition takes place at the reactor outlet ( $T_3$ ), where temperature rises first and methane concentration is still relatively high. Once the reaction has ignited, a drastic increase in methane conversion is observed with almost complete selectivity to  $\text{CO}_2$ , while the reaction front moves backwards, with

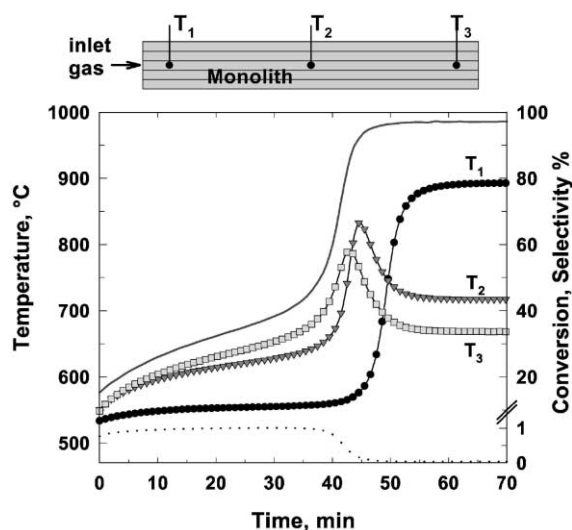


Fig. 1. Typical solid temperature profiles at three different axial positions (●,  $T_1$ ; ▼,  $T_2$ ; □,  $T_3$ ), methane conversion (—) and selectivity to carbon monoxide (···) as functions of time over  $\text{LaMnO}_3/\text{La-}\gamma\text{-Al}_2\text{O}_3$  monolith aged 20 h under reaction. Inlet gas temperature:  $525^\circ\text{C}$ ;  $L = 4.6\text{ cm}$ ; gas flow rate, 48  $\text{NL/h}$ . Feed:  $\text{CH}_4$  (3 vol.%);  $\text{O}_2$  (10 vol.%);  $\text{N}_2$  balance.

temperature profiles shifting their maximum from outlet to inlet sections of the monolith. This behaviour appears to be significantly different from that usually reported in both experimental and modelling results of

$\text{PdO}$ -based monolithic reactors for methane combustion, showing light-off near the entrance with the heat wave being propagated towards the reactor exit [13].

At steady-state, methane is almost completely converted in the first zone of the reactor, with the remaining part working as a heat exchanger (which cools the hot gas), determining large differences in catalyst temperatures and strong axial gradients.

The temperature rise on the catalyst surface is a strong function of the flow rate of reactants. Fig. 2 shows the behaviour of  $T_1$  temperature (temperature measured at 0.5 cm from monolith entry, i.e. the hottest part of catalyst in ignited conditions) at three different gas flow rates values as a function of time in dynamic experiments carried out by raising the gas preheating temperature at a rate of  $4^\circ\text{C}/\text{min}$ . As total conversion of methane with complete selectivity to  $\text{CO}_2$  is always reached in ignited conditions, independently of gas flow rate, the transient evolution of temperature profiles could be used as useful indicator of the chemical and physical processes occurring in the catalyst.

The influence of flow rate on the minimum ignition temperature is negligible (Fig. 2), while temperature levels reached by the catalyst result are significantly affected. At the highest flow rate value investigated, temperature of catalyst entry section rises up to about  $1000^\circ\text{C}$ , while feeding the reactant mixture at a rate three times lower (24  $\text{NL/h}$ ) results in a slower increase

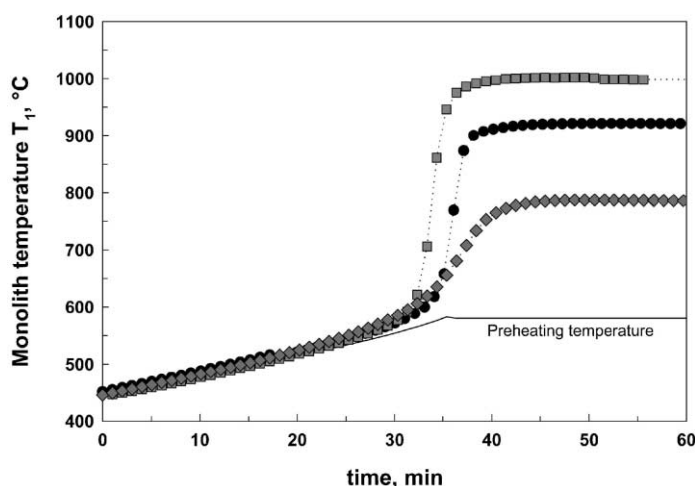


Fig. 2. Catalyst temperature  $T_1$  (0.5 cm from inlet) as a function of time in methane combustion over  $\text{LaMnO}_3/\text{La-}\gamma\text{-Al}_2\text{O}_3$  monolith 4.6 cm long at different feed flow rates: (◆) 24, (●) 48, (■) 72  $\text{NL/h}$ . Feed:  $\text{CH}_4$  (3 vol.%);  $\text{O}_2$  (10 vol.%); balance  $\text{N}_2$ .

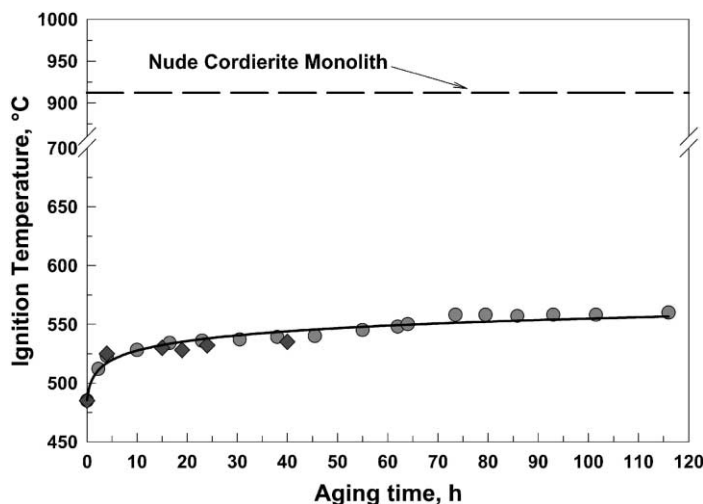


Fig. 3. Minimum ignition temperature in methane combustion measured over  $\text{LaMnO}_3/\text{La}-\gamma\text{-Al}_2\text{O}_3$  monolithic catalysts of different lengths: (◆) 4.6 cm, (●) 2.3 cm. Feed:  $\text{CH}_4$  (3 vol.%);  $\text{O}_2$  (10 vol.%); balance  $\text{N}_2$ . Flow rate: 48 NL/h.

of solid temperature up to only  $790^\circ\text{C}$ . This happens because at higher rates a larger power is produced by combustion, and consequently, a higher temperature gradient must be established between catalyst walls and surroundings to disperse it. It is worth noting that the independence of ignition point on gas flow rate suggest a kinetic activation of the phenomenon not affected by the gas-catalyst mass transfer resistance at lower temperature.

The effect of catalyst length has been investigated by carrying out combustion experiments on a shorter sample (length 2.3 cm). Results are presented in Fig. 3, where the comparison between shorter and longer monoliths is performed in terms of minimum ignition temperature values measured as a function of ageing time under reaction. No major difference can be detected in terms of ignition temperature, suggesting that the steady-state light-off point is near the reactor inlet with the remaining part of the reactor behaving as a heat exchanger.

Fresh catalysts were only pretreated at  $800^\circ\text{C}$  before combustion experiments, therefore, deactivation occurs after exposure to higher temperatures and steam generated during reaction. In a previous investigation, we showed that 6 h ageing under combustion at  $1100^\circ\text{C}$  deactivates the catalyst up to a stable and still very active state. In this case, exposure at ignited conditions of catalysts means they undergo a slightly

weaker thermal treatment at about  $1000^\circ\text{C}$  maximum temperature, so a longer time is needed to reach a stable stationary regime. However, after about 60 h working time, ignition temperature levels off to a constant value,  $350^\circ\text{C}$  lower than that required on a nude cordierite monolith tested under same experimental conditions. Catalyst durability tested up to 120 h of operation under reacting condition results strongly enhanced with respect to previously reported perovskite-based monoliths [9].

The catalytic combustor can exhibit a steady-state multiplicity typical of highly exothermic reactions, as reported by other authors both experimentally [14] and theoretically [15]. Fig. 4 shows that at least two stable steady-states exist, resulting in different values of the ignition and extinction temperatures with a hysteresis of about  $55^\circ\text{C}$ .

The experimental runs reported in Fig. 4 have been performed by first raising the inlet gas temperature from a low conversion condition up to an ignited condition (ignition path) and subsequently decreasing it progressively to blow-out the reaction (extinction path). Results are reported in terms of overall methane conversion, CO production and solid temperatures attained in steady-state conditions as functions of inlet gas temperature. With increasing inlet gas temperature, the methane conversion increases slowly before the ignition and then much more steeply at light-off,

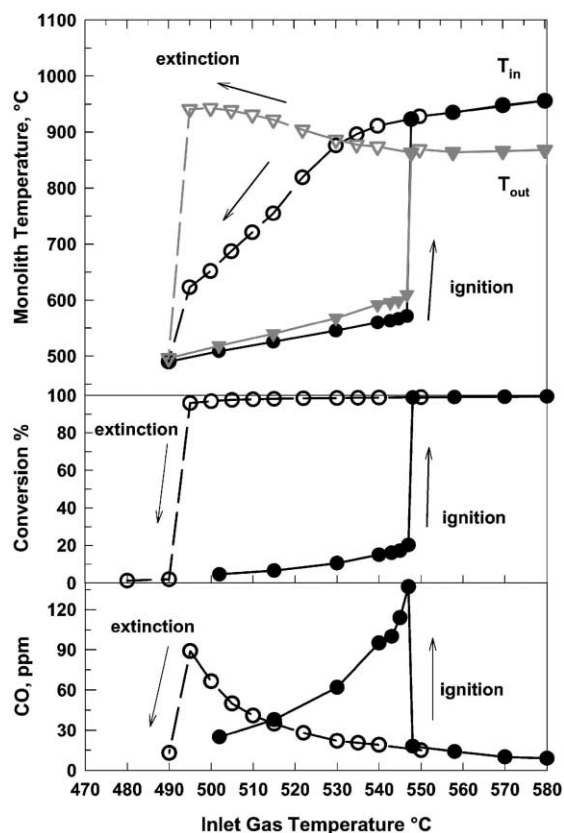


Fig. 4.  $T_{in}$  (0.5 cm from the inlet) and  $T_{out}$  (0.8 cm from the outlet) catalyst temperatures, methane conversion and CO yield as functions of inlet gas temperature in a steady-state ignition–extinction cycle over a  $\text{LaMnO}_3/\text{La}-\gamma\text{-Al}_2\text{O}_3$  monolith 2.3 cm long, aged for 64 h. Flow rate: 48 Nl/h. Feed:  $\text{CH}_4$  (3 vol.%);  $\text{O}_2$  (10 vol.%); balance  $\text{N}_2$ .

where quite a step change of total conversion is observed by heating the gas from 545 to 547°C. Simultaneously, measurements of solid temperatures show a profile with maximum close to the end of the reactor just before ignition, while as already reported in Fig. 1, at steady-state ignited conditions, the maximum is positioned close to the reactor entrance. Conversely, by decreasing the preheating temperature, before achieving blow-out conditions at 490°C, the reaction front progressively moves towards the end of the reactor as confirmed by the inversion between catalyst temperature values  $T_{in}$  and  $T_{out}$  recorded in the extinction branch (Fig. 4). It is worth noting that

CO production is very low under ignited conditions regardless of the long ageing of the catalyst, and tends to increase only due to homogeneous contribution in the post-catalytic zone when the hot exit gas still contains some unreacted methane (i.e. just before light-off and blow-out).

### 3.1. Model development

A heterogeneous mono-dimensional model has been developed on the basis of the following assumptions:

1. Gas phase axial diffusion is neglected (Peclet number is higher than 150).
2. Gas phase energy balance is written in steady-state because of the higher solid thermal capacity compared to the gas thermal capacity,  $\rho_s c_p s \gg \rho_g c_p g$ .
3. Mass balance equations are written in steady-state.
4. Fully developed laminar flow.
5. Homogeneous reaction is neglected.
6. The channels have been assumed at thermal equilibrium along the radial direction the inlet conditions being uniform and radial heat transfer time much lower than the convection time ( $vd^2/\alpha L \approx 1000$ ).
7. No mass and energy resistances have been considered through the catalyst layer, Prater number and Thiele modulus being much lower than 1.
8. In order to take into account the thermocouple lag, the effective thickness of the channel has been increased by a factor  $1/\delta$  [16].
9. The gas phase properties are variable with temperature and assimilated to those of air.

### 3.2. Model equations

Gas phase mass balance,  $\text{CH}_4$ :

$$v_g \left( \frac{dx_{\text{CH}_4}}{dz} \right) = -k_g a_v (x_{\text{CH}_4} - x_{\text{CH}_4}^s) \quad (1)$$

Boundary condition:

$$\text{at } z = 0 \quad x_{\text{CH}_4} = x_{\text{CH}_4}^{\text{in}} \quad (1a)$$

Solid phase mass balance,  $\text{CH}_4$ :

$$k_g a_{v,s} (x_{\text{CH}_4} - x_{\text{CH}_4}^s) = R_{\text{CH}_4} \quad (2)$$

Gas phase energy balance:

$$v_g \rho_g C_{p_g} \left( \frac{dT_g}{dz} \right) = -h_g a_v (T_g - T_s) \quad (3)$$

Boundary condition:

$$\text{at } z = 0, \quad T_g = T_g^{\text{in}} \quad (3a)$$

Solid phase energy balance:

$$\begin{aligned} \rho_s C_{p_s} \left( \frac{\partial T_s}{\partial t} \right) &= \lambda_s \left( \frac{\partial^2 T_s}{\partial z^2} \right) + \delta h_g a_{v,s} (T_g - T_s) \\ &+ \delta \Delta H_{\text{RCH}_4} C_g + \delta \sigma \varepsilon a_{\text{rad}} (T_w^4 - T_s^4) \\ &+ U_s (T_w - T_s) \end{aligned} \quad (4)$$

Initial condition:

$$t = 0, \quad T_s = T_s^0 \quad (4a)$$

Boundary conditions:

$$\text{at } z = 0, \quad \lambda_s \frac{\partial T_s}{\partial z} = \sigma \varepsilon (T_s^4 - T_w^4) \quad (4b)$$

$$\text{at } z = L, \quad -\lambda_s \frac{\partial T_s}{\partial z} = \sigma \varepsilon (T_s^4 - T_w^4) \quad (4c)$$

As the monolith is covered by ceramic wool and surrounded by a quartz tube inserted in an electrical furnace, another energy balance must be considered, which takes into account the heat capacity of both quartz and ceramic wool. We have named “wall” this new entity, evaluating the heat flux across it in unsteady-state conditions written as follows:

Wall energy balance:

$$\begin{aligned} \rho_w C_{p_w} \left( \frac{\partial T_w}{\partial t} \right) &= -U_{wF} (T_w - T_F) - \sigma \varepsilon a_w (T_w^4 - T_s^4) \\ &- U_w (T_w - T_s) - \sigma a_{wF} (T_w^4 - T_F^4) \end{aligned} \quad (5)$$

Initial condition:

$$t = 0, \quad T_w = T_w^0 \quad (5a)$$

The system of partial differential equations (1)–(5) with the boundary conditions (1a), (3a), (4b) and (4c) and the initial conditions (4a) and (5a) has been first reduced to a system of ordinary differential equations.

Table 1

Parameters values in the simulation

$d$ (m)	$1.086 \times 10^{-3}$
$L$ (m)	$4.6 \times 10^{-2}$
$T_f$ (K)	760
$T_g^{\text{in}}$ (K)	760
Inlet $v_g$ (m/s)	1.5
$\delta$	0.65
$\varepsilon$	0.75
$\rho_s$ (kg/m <sup>3</sup> )	2400
$\lambda_s$ (W/m K)	3
$C_{p_s}$ (J/(kg K))	$1050 + 0.1 T_s$

The resulting system has been solved at each time step by using a Delphi routine based on the Crout algorithm.

Parameters used in simulations (Table 1) have been chosen from laboratory measurements and literature references. The effective solid conductivity ( $\lambda_s$ ) and the solid emissivity ( $\varepsilon$ ) have been used as fitting parameters in order to reproduce respectively reaction front movement and the overall heat loss from catalyst to outside.

In mono-dimensional models, simulation results are strongly dependent on the value of heat and mass transfer coefficients [17]. In our model, correlations proposed by Hawthorn [18] in the absence of reaction have been used to calculate  $Nu$  and  $Sh$  numbers. More interesting expressions derived by Ullah et al. [19] and Bennett et al. [20] in reacting conditions and concerning the light-off point suffer from significant errors, due to the presence of not completely mass transfer controlled regime as pointed out by Hayes and Kolaczowski [21]. However, our choice is justified by the lower activity of perovskites compared to Pd-based catalysts, which prevents a sharp transition from kinetically to mass transfer limited regimes at light-off usually associated to the largest discrepancy of  $Nu$  and  $Sh$  numbers from their asymptotic values [17]. Correctness of this hypothesis is presently under investigation.

### 3.3. Model simulations and comparison with the experimental results

Model was run in order to simulate transient experiments conducted over a fresh 4.6 cm long catalyst both before ignition and during the first light-off, since kinetic characterisation is available in these

conditions and activity can be considered uniform along the monolith. Previous studies under isothermal conditions [11] allowed to describe combustion kinetics over the same fresh catalyst by means of the following rate equation:

$$R_{\text{CH}_4} = 1260 \exp\left(-\frac{E_{\text{act}}}{RT}\right) x_{\text{CH}_4}^{0.8} \rho_s \quad (6)$$

with

$$E_{\text{act}} = 18,200 \text{ cal/mol} \quad (6a)$$

Model simulations at steady-state (not shown) reproduce well the steep conversion plots obtained over the fresh perovskite-based monolith as a function of preheating temperature [11] with good agreement on the minimum ignition temperature (485°C). Fig. 5a shows the transient temperature profiles during first light-off as obtained by the model in comparison with the experimental values measured in three axial positions of the monolith. It turns out that during the

transient phase, the catalyst reaches temperature values higher than the steady-state ones with a reaction front which moves from the outlet towards the inlet of the channel in a time scale seven orders of magnitude higher than the residence time. The agreement between experimental and model results has been obtained by varying the solid thermal conductivity up to an optimal value of 3 W/m K which gives a characteristic time ( $L^2/\alpha = 1000$  s) of the same order of magnitude as the time taken by the heat wave to move into the monolith. The obtained value of  $\lambda_s$  is reasonable when compared with typical values of the cordierite support [22] and slightly increased to take into account the internal channel radiant heat flux [23].

It is worth noting that the longer transient measured before ignition over the 20 h aged catalyst (Fig. 1) with respect to the fresh monolith (Fig. 5a) is basically related to the change of catalytic reaction rate, as confirmed by the increase in minimum preheating temperature required for light-off (525 vs. 485°C).

Fig. 5b shows the spatial temperature profile expected by the model at steady-state. The light-off stabilises in a small region in the vicinity of the reactor entrance and the final part behaves as an heat exchanger being involved in the reaction only in the transient (methane conversion is almost complete after the light-off point). The estimated value of  $\varepsilon$  (0.75), entirely determined by the whole energy loss from the catalyst (the temperature rise is lower than adiabatic) allows us also to obtain a satisfactory reproduction of the axial temperature gradient in the solid at steady-state. On the other hand, gas temperature profile along the channel resembles similar patterns showed in most recent modelling results [16], with the typical inversion in the direction of heat transfer related to the crossover between gas and solid temperatures downstream of light-off point.

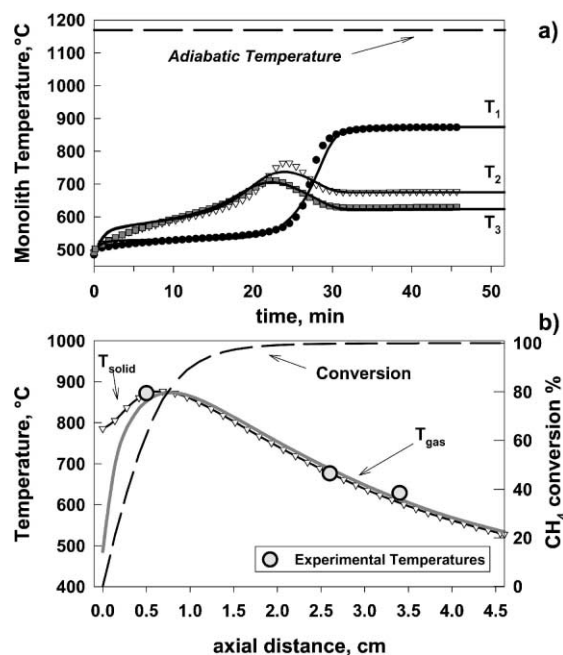


Fig. 5. Comparison between model and experimental temperature profiles over a fresh monolithic catalyst: (a) during transient ignition; (b) along the reactor at steady-state.  $L = 4.6$  cm; inlet gas temperature, 485°C; gas flow rate, 48 Nl/h. Feed:  $\text{CH}_4$  (3 vol.%);  $\text{O}_2$  (10 vol.%);  $\text{N}_2$  balance.

#### 4. Conclusions

Perovskite-based catalysts prepared via active phase dispersion on  $\text{La}/\gamma\text{-Al}_2\text{O}_3$  porous washcoat deposited on cordierite monoliths are active and stable in methane combustion up to at least 1000°C. A  $\text{CH}_4/\text{O}_2/\text{N}_2$  mixture is completely converted to  $\text{CO}_2$  and  $\text{H}_2\text{O}$  provided its inlet temperature is at about 500°C, a value not influenced by catalyst length and



gas flow rate. Gas flow rate significantly affects solid steady-state temperature, as at higher flow rates the system becomes more adiabatic. A weak deactivation of catalysts is observed in the initial operations, while after 120 h under reaction conditions, the activity appears stable and still very high. The transient behaviour of the system during start-up and/or blow-off conditions is characterised by reaction front movement, from the outlet to the inlet monolith sections (ignition) or vice versa (extinction), whose time scale has been reproduced by a kinetic model, characterised by an increased solid thermal conductivity to take into account the significant contribution of radiation inside channels, and by strong radiant heat transfer with the surroundings.

### Acknowledgements

Authors wish to kindly acknowledge financial support from ENEL PTE and MURST (Rome, Italy).

### References

- [1] P. Forzatti, G. Groppi, *Catal. Today* 54 (1999) 165.
- [2] H. Sadamori, *Catal. Today* 47 (1999) 325.
- [3] G. Saracco, I. Cerri, V. Specchia, R. Accornero, *Chem. Eng. Sci.* 54 (1999) 3599.
- [4] S. Ro, A. Scholten, *Catal. Today* 47 (1999) 415.
- [5] B. Emonts, *Catal. Today* 47 (1999) 407.
- [6] M.F.M. Zwinkels, S.G. Jaras, P.G. Menon, in: A. Cybulski, J. Moulijn (Eds.), *Structured Catalysts and Reactors*, Marcel Dekker, New York, 1998, p. 149.
- [7] L.G. Tejuca, J.L.G. Fierro, J.M.D. Tascon, *Adv. Catal.* 36 (1989) 237.
- [8] H. Arai, T. Yamada, K. Eguchi, T. Seyama, *Appl. Catal.* 26 (1986) 265.
- [9] H. Arai, M. Machida, *Appl. Catal. A* 138 (1996) 161.
- [10] S. Cimino, R. Pirone, L. Lisi, M. Turco, G. Russo, *Catal. Today* 59 (2000) 19.
- [11] S. Cimino, R. Pirone, G. Russo, *Ind. Eng. Chem. Res.* 40 (2001) 80.
- [12] A. Boehman, *AIChE J.* 44 (1998) 2745.
- [13] R. Wanker, H. Raupenstrauch, G. Staudinger, *Chem. Eng. Sci.* 55 (2000) 4709.
- [14] R. Prasad, H.L. Tsai, L.A. Kennedy, E. Ruckenstein, *Combust. Sci. Technol.* 26 (1981) 51.
- [15] R.E. Hayes, S.T. Kolaczowski, *Chem. Eng. Sci.* 49 (1994) 3587.
- [16] R.E. Hayes, S.T. Kolaczowski, J. Thomas, J. Titiloye, *Ind. Eng. Chem. Res.* 35 (1996) 406.
- [17] G. Groppi, E. Tronconi, P. Forzatti, *Catal. Rev.-Sci. Eng.* 41 (1999) 227.
- [18] R.D. Hawthorn, *AIChE Symp. Ser.* 70 (1974) 428.
- [19] U. Ullah, S.P. Waldrum, C.J. Bennett, T. Truex, *Chem. Eng. Sci.* 47 (1992) 2413.
- [20] C.J. Bennett, S.T. Kolaczowski, W.J. Thomas, *Trans. IChemE B* 69 (1991) 209.
- [21] R.E. Hayes, S.T. Kolaczowski, *Chem. Eng. Sci.* 49 (1994) 3587.
- [22] R.E. Hayes, S.T. Kolaczowski, *Introduction to Catalytic Combustion*, Gordon and Breach, Amsterdam, 1997.
- [23] S.-T. Lee, R. Aris, *Chem. Eng. Sci.* 32 (1977) 827.